

m6A regulator-based methylation modification patterns and characterization of tumor microenvironment in acute myeloid leukemia

Zi-jun Xu

Affiliated People's Hospital of Jiangsu University

Xiang-mei Wen

Affiliated People's Hospital of Jiangsu University

Yuan-cui Zhang

The Affiliated Third Hospital of Jiangsu University

Ye Jin

Affiliated People's Hospital of Jiangsu University

Ji-chun Ma

Affiliated People's Hospital of Jiangsu University

Yu Gu

Affiliated People's Hospital of Jiangsu University

Xin-yi Chen

Affiliated People's Hospital of Jiangsu University

Pei-hui Xia

Affiliated People's Hospital of Jiangsu University

Wei Qian

Affiliated People's Hospital of Jiangsu University

Jiang Lin

Affiliated People's Hospital of Jiangsu University

Jun Qian (✉ qianjun0007@hotmail.com)

Affiliated People's Hospital of Jiangsu University

Research Article

Keywords: m6A, acute myeloid leukemia, tumor microenvironment, immune infiltration, metabolic pathways

Posted Date: May 13th, 2022

DOI: <https://doi.org/10.21203/rs.3.rs-1627972/v1>

License:  This work is licensed under a Creative Commons Attribution 4.0 International License.

[Read Full License](#)

Abstract

RNA N6-methyladenosine (m6A) is the most common and intensively studied RNA modification that critically regulates RNA metabolism, cell signaling, cell survival, and differentiation. However, the overall role of multiple m6A regulators in the tumor microenvironment (TME) has not yet been fully elucidated in acute myeloid leukemia (AML). In our study, we explored the genetic and transcriptional alterations of 23 m6A regulators in AML patients. Three distinct molecular subtypes were identified and associated with prognosis, patient clinicopathological features, as well as TME characteristics. The TME characterization revealed that m6A patterns were highly connected with metabolic pathways such as biosynthesis of unsaturated fatty acids, cysteine and methionine metabolism, and citrate cycle TCA cycle. Then, based on the differentially expressed genes (DEGs) related to m6A molecular subtypes, our study categorized the entire cohort into three m6A gene clusters. Furthermore, we constructed the m6A score for quantification of the m6A modification pattern of individual AML patients. It was found that the tumor-infiltrating lymphocyte cells (TILs) closely correlated with the three m6A clusters, three m6A gene clusters, and m6Ascore. And many signaling pathways were involved, including glycogen degradation, drug metabolism by cytochrome P450, pyruvate metabolism, and so on. Our comprehensive analysis of m6A regulators in AML demonstrated their potential roles in the clinicopathological features, prognosis, tumor microenvironment, and particularly metabolic pathways. These findings may improve our understanding of m6A regulators in AML and offers new perspectives on the assessment of prognosis and the development of anticancer strategy.

Introduction

Acute myeloid leukemia (AML) is a highly fatal hematopoietic malignancy with excessive proliferation of immature leukemic blasts and poor prognosis [1, 2]. The recurrence and mortality rates of AML are still very high with currently available therapeutics [3, 4]. The scientists have been dedicated to developing more novel and synergistic therapeutic targets of AML [5]. A lot of work has been done on the role of gene transcription in leukemogenesis whereas the functional significance of posttranscriptional regulation of gene expression such as RNA modifications has received great attention from researchers in recent years.

Methylation of N6 adenosine (m6A), which has been discovered as reversible RNA methylation affecting the regulation of post-transcriptional gene expression programs and protein production, is one of the most abundant internal marks on mammalian mRNA [6–9]. The biological functions of m6A are dynamically controlled by the m6A methyltransferase complex (writers), m6A demethylases (erasers), and m6A-binding proteins (readers) [6, 10]. A deep understanding of these regulatory proteins is essential to our comprehension of the mechanisms of m6A in gene regulation. It has been reported that m6A modification is an important regulator of the development and regulation of normal and malignant hematopoiesis [11]. Emerging evidence also demonstrates the involvement of m6A modification in physiological and pathological processes of hematopoiesis and leukemogenesis [12, 13]. The m6A writers [methyltransferase-like 3 (METTL3), methyltransferase-like 14 (METTL14)], erasers [α -ketoglutarate-dependent dioxygenase AlkB homolog 5 (ALKBH5), and fat mass and obesity-associated

protein (FTO)], highly expressed in AML, involved in the development, differentiation, progression, and maintenance of AML through various m6A-dependent mechanisms [14–18]. m6A reader gene YT521-B homology (YTH) domain family protein 2 (YTHDF2) is also upregulated and plays an important role in tumor promotion in AML development/maintenance [13].

The tumor microenvironment (TME), a complex ecosystem that includes malignant and non-malignant cells, immune cells, stromal cells, and other components, plays a crucial role in tumor initiation and progression [19–21]. Also, cancer cells autonomously alter their metabolic pathways since they need abundant energy and raw materials required for proliferation and survival [20, 22]. The researchers show that the modification of m6A is also implicated in the regulation of physiology and metabolism in tumors [23, 24]. Leukemia-associated alterations within the AML niche such as increased hypoxia, inflammation and metabolic reprogramming facilitate immune evasion and chemotherapy resistance as well as contribute to AML progression [25]. Liu et al manifest that the m6A demethylase FTO can regulate glycolytic metabolism which induces tumors to escape immune surveillance [26]. Nevertheless, most studies focus on only individual or small numbers of m6A regulators due to technical limitations. How multiple m6A regulators mediate the micro-environmental phenotype which may provide important insights for understanding the underlying mechanism of AML tumorigenesis is not well elaborated.

In this study, we obtained the datasets of AML from the Cancer Genome Atlas (TCGA). Next, we constructed the three m6A clusters, three m6A gene clusters, and a set of scoring system step by step and comprehensively evaluated the association of m6A modification patterns with clinical outcomes, biological pathways, and TME characteristics. All in all, we attempt to uncover the mechanism of m6A modification patterns in the AML development, and subsequently provide references for future research and a basis for clinical treatment.

Materials And Methods

Data acquisition

Public gene expression with clinicopathological data was downloaded from the GDC of the TCGA portal (<https://portal.gdc.cancer.gov/repository>). Patients without survival information were excluded and a total of 151 AML patients were included for further evaluation. Somatic gene mutations with clinical data were also obtained (n=193) and analyzed with R package 'maftools'.

Consensus molecular clustering for 23 m6A regulators

A total of 23 acknowledged m6A regulators were analyzed for identifying different m6A modification patterns. These 23 m6A regulators comprised 2 erasers (ALKBH5, FTO), 13 readers (YTHDC1, YTHDC2, YTHDF1, YTHDF2, YTHDF3, IGF2BP1, IGF2BP2, IGF2BP3, HNRNPA2B1, HNRNPC, FMR1, LRPPRC, ELAVL1), and 8 writers (METTL3, METTL14, RBM15, RBM15B, WTAP, VIRMA, CBLL1, ZC3H13). We applied the R package "ConsensusClusterPlus" to classify patients into distinct m6A modification patterns according to the expression of 23 m6A regulators. Next, we compared the relationships between

m6A molecular subtypes and clinicopathological characteristics including FAB subtypes, cytogenetic risk, gender, age, and WBC.

DEGs identification

m6A modification-related differentially expressed genes (DEGs) were checked among different m6A subtypes using the empirical Bayesian approach of the limma R package. We categorized the cases into different subtypes (gene cluster A, gene cluster B, and gene cluster C) for further analysis. In practice, we used the voom algorithm to normalize gene expression data and then input lmFit and eBayes functions to calculate the statistics for differential expression with a corrected P -value < 0.05 . GO annotation for m6A phenotype-related genes was performed in the R package 'clusterProfiler' with the cutoff value of FDR < 0.05 . Kaplan-Meier curves analysis was employed to measure the discrepancy of overall survival (OS) between different gene clusters.

Generation of m6A gene signature

The m6AScore was set up to assess the m6A modification patterns of individual patients with AML by using principal component analysis (PCA). To be more specific, a total of 70 overlap DEGs were subjected to univariate Cox regression analysis to identify a set of candidate prognostic genes. And we screened out 25 genes with a P value less than 0.05 by the random forest-recursive feature elimination (RFE) method with 10-fold cross-validation in the R package 'caret'. Then we conducted the PCA analysis based on the expression profiles of the final determined genes. Principal components 1 and 2 were both selected as signature scores. As a result, the m6AScore was calculated as follows: $m6AScore = \Sigma(PC1_i + PC2_i)$ [27]. m6AScore was the integral of a continuous variable and the m6AScore group was a binary variable obtained according to the X tile method.

Gene set variation analysis (GSVA) and TME cell infiltration estimation

We employed GSVA enrichment analysis to evaluate the disparity involved in physiological processes and biological functions among different m6A modification patterns by using 'GSVA' R packages. Additionally, we adopted the CIBERSORT algorithm to calculate the relative abundance of 23 tumor-infiltrating lymphocyte cells (TILs) in different m6A modification patterns with the gene expression profile [28]. And the 23 cell types included B cells, T cells, dendritic cells, natural killer cells, eosinophil, macrophages, monocyte, neutrophil, and myeloid subsets. A violin map visualized the difference of immune cell abundance among m6A modification patterns. To extract detailed mutational information, Mutation Annotation Format data files based on TCGA cohort were depicted by the waterfall function of the R 'maftools' package.

Statistical analyses

We generated statistical analyses in this study with R software version 4.0.4 (<https://www.r-project.org/>). For comparison of two continuous variables, statistical significance was evaluated by the Chi-square test and Fisher's exact test. Univariate Cox regression and Kaplan-Meier curves were used to test the

prognostic effects of the different subtypes with the “survival” and “survminer” R packages. Samples were allocated into high and low m6AScore subgroups with the surv-cutpoint function from the ‘survminer’ package. The two-sided $P < 0.05$ in all comparisons was considered to indicate a statistically significant difference.

Results

Genetic and transcriptional alterations of m6A regulators in AML

We investigated a total of 23 m6A regulators including 8 writers, 2 erasers, and 13 readers in this study (Table S1). The differences in copy number variation (CNV) of all regulators were explored. The CNV of m6A regulators was prevalent in AML. The CNV was found to be focused on the deletion predominantly, while YTHDF2, YTHDF3, FTO, YTHDF1, and ELAVL1 had more prevalent amplification frequency (Figure 1A, Table S2). The locations of CNV alteration in 23 m6A regulators on their respective chromosomes were displayed in Figure 1B (Table S3, Table S4). Moreover, we compared AML samples to normal samples using PCA analysis based on paired tumor-normal specimens and found that AML samples were clearly distinguished from normal samples by the 23 m6A regulators (Figure S1A). After evaluating the incidence of somatic mutations of 23 m6A regulators in AML, we concluded that the alteration frequency was only 1.04% among 193 samples with 2 missense mutations identified in METTL3 and RBMX (Figure 1C). Notably, m6A regulators are widely known for their collaboration in cancer progression. The relevance of the co-expression of regulators was therefore analyzed, and LRPPRC and VIRMA owned a significant correlation with the highest correlation coefficient ($R = 0.66$) (Figure 1D, Table S5 and Table S6). Intrigued by these findings, we further compared the mRNA expression levels between AML and normal tissues. The results displayed all of the 23 m6A regulators showed significant differences between AML and normal tissues except for YTHDF2 and METTL3 (Figure 1E). Beyond that, m6A highlighted distinct patterns in different immune cell types, myeloid malignancies along with lymphoid malignancies (Figure S1B, Figure S1C). The observed clustering suggested that the cell-of-origin and different disease groups influenced the repertoire of m6A regulators. YTHDF3 presented relatively higher expression compared with the other 22 m6A regulators in M2-macrophage. At the same time, AML highly expressed IGF2BP2.

Identification of m6A subtypes in AML

151 patients from the TCGA dataset with available OS data and clinical information were enrolled in our study for further analysis (Table S7). The results of univariate Cox regression analysis revealed the prognostic values of 23 m6A regulators in patients with AML (Table S8). Figure 2A showed the comprehensive landscapes of 23 m6A regulators concerning their interactions, connections, and prognostic values in AML in the form of a m6A regulator network. Significant correlations existed among writers, erasers, and readers. We further explored the expression pattern of m6A regulators in AML and conducted the R package of ConsensusClusterPlus to classify the patients based on the expression level of 23 m6A regulators. It was clear that the clustering model was optimal when $K = 3$ during the process of

K ranging from 2 to 9 (Figure S2A- S2C). The entire cohort was eventually allocated into three distinct modification patterns consisting of 111 cases in cluster A, 33 cases in cluster B, and 7 cases in cluster C (Figure 2B). The Kaplan-Meier curves for the three main m6A modification subtypes revealed the worst overall survival in patients with m6A cluster A ($P = 0.003$, Figure 2B). The prognosis of m6A cluster-B and m6A cluster C was similar in the Kaplan-Meier analysis, so we combined m6A cluster B with m6A cluster C and m6A cluster A was compared with it using univariate analyses. m6A cluster A had significantly poorer prognosis (HR = 0.3998, $P < 0.01$, Table S9). Moreover, we validated the biological characteristics of three m6A subtypes. The m6A cluster B was preferentially related to FAB subtypes M3, and the m6A cluster C subtype was markedly correlated with intermediate cytogenetic risk and FTO (Figure 2C).

Associations of TME with three m6A subtypes

The association of 23 TILs with three m6A clusters was investigated by using the CIBERSORT algorithm in the TME of AML. We observed profound differences in immune cell infiltration including activated B cell, CD56dim natural killer cell, immature B cell, mast cell, regulatory T cell, type 1 T helper cell, type 17 T helper cell, and type 2 T helper cell among the three subtypes (Figure 3A). In addition, we performed GSVA enrichment analysis to detect the biological characteristics of three distinct m6A modification patterns. GSVA enrichment analysis showed that m6A cluster A was significantly enriched in metabolic pathways such as biosynthesis of unsaturated fatty acids, propanoate metabolism, pyruvate metabolism, citrate cycle TCA cycle, glyoxylate and dicarboxylate metabolism, pyrimidine metabolism, purine metabolism, cysteine and methionine metabolism (Figure 3B and Table S10). m6A cluster B presented enrichment pathways highly related to metabolic pathways including linoleic acid metabolism (Figure 3B and Table S10), and carcinogenic activation pathways such as ECM receptor interaction (Figure 3C and Table S11). Likewise, m6A cluster C was prominently associated with metabolic pathways which encompassed cysteine and methionine metabolism, glyoxylate and dicarboxylate metabolism (Figure 3C and Table S11). What's more, m6A cluster A correlated with immune pathways and immune-related diseases simultaneously, including antigen processing and presentation, chemokine signaling pathway activation, asthma, and systemic lupus erythematosus (Figure 3D and Table S12). Figure 3E illustrated cell type assignment for the scRNA expressed genes in AML.

m6A phenotype-related DEGs in AML

To further investigate the underlying m6A-related transcriptional expression differences within three m6A modification patterns, we did some further analysis. Actually, we applied a Venn diagram to illustrate the DEGs among the three m6A modification patterns and 70 m6A phenotype-related overlap genes were presented (Figure S3A, Table S13-S16). To further elaborate on the function of DEGs, we carried out a GO enrichment analysis. The result elucidated that enrichment of the biological processes related to embryonic organ morphogenesis/development (Figure S3B). Table S17 showed the expression level of 70 overlap DEGs. Univariate Cox regression study of 70 genes was analyzed and 25 genes with P -value less than 0.05 were screened out (Table S18). Then we performed an unsupervised clustering algorithm to classify the entire cohort into three m6A gene signature subtypes, named as m6A gene cluster A-C,

respectively (Figure 4A). Further survival analysis indicated three m6A genomic phenotypes showed significant prognostic differences in AML samples, of which 45 cases were in gene cluster A, 47 cases in gene cluster B, and 59 cases in gene cluster C ($P = 0.002$, Log-rank test, Figure 4B). Patients in gene cluster C were proved to be related to a better prognosis, while patients in gene cluster A and gene cluster B were associated with the outcome of poorer prognosis. We also observed that m6A gene cluster C patterns were associated with good cytogenetic risk, while m6A gene cluster A presented poor cytogenetic risk and m6A gene cluster B showed intermediate cytogenetic risk. Patients with alive status were largely concentrated in the m6A gene cluster A patterns. Interestingly, VSTM1 and M1AP were markedly decreased in the m6A gene cluster B and increased in the m6A gene cluster C (Figure 4C). The three m6A gene clusters indicated significant differences in the expression of VIRMA, IGF2BP2, FMR1, IGF2BP3, ELAVL1, and YTHDC2 (Figure 4D).

In addition, the immune cell infiltration of activated B cell, activated CD4 T cell, activated dendritic cell, macrophage, NK cell, plasmacytoid dendritic cell and type 2 T helper cell showed statistically significant differences across the three m6A gene clusters (Figure 5A). Meanwhile, m6A gene cluster A was prominently associated with metabolic pathways including mucin type O glycan biosynthesis, nitrogen metabolism, heme biosynthesis, lysine degradation, epinephrine biosynthesis, glycogen degradation, pantothenate and CoA biosynthesis, vitamin B6 metabolism, retinoic acid metabolism, phenylalanine tyrosine and tryptophan biosynthesis (Figure 5B, Figure 5C and Table S19, Table S20). m6A gene cluster B was enriched in the pathway associated with retinoid metabolism, glyoxylate and dicarboxylate metabolism, steroid biosynthesis, nicotinamide adenine dinucleotide biosynthesis, ubiquinone, and other terpenoid quinone biosynthesis, folate biosynthesis, oxidative phosphorylation, glycogen degradation, cysteine and methionine metabolism, phenylalanine tyrosine and tryptophan biosynthesis, pantothenate and CoA biosynthesis, pentose phosphate, primary bile acid biosynthesis, and retinoic acid metabolism (Figure 5C, Figure 5D, and Table S20, Table S21). m6A gene cluster C presented enrichment pathways prominently associated with retinol metabolism, ascorbate and aldrate metabolism, steroid hormone biosynthesis and metabolism, porphyrin and chlorophyll metabolism, metabolism of xenobiotics by cytochrome P450, drug metabolism by cytochrome P450, epinephrine biosynthesis, lysine degradation, and N glycan biosynthesis (Figure 5C, Figure 5D, and Table S20, Table S21).

Construction of m6A score and the relevance of clinical features.

Considering the individual heterogeneity and complexity of m6A modification, a scoring system based on the signature genes related to m6A, named m6AScore, was established to quantify the m6A modification pattern of single AML patient (Table S22). Figure 6A illustrated an alluvial diagram of three m6A clusters, three m6A gene clusters, m6AScore, and OS status. Remarkably, m6A cluster B exhibited the highest m6A score, followed by m6A cluster A and m6A cluster C (Figure S4A). The results suggested that the m6AScore of m6A gene cluster B was the lowest, while that of m6A gene cluster C was the highest (Figure S4B). Spearman analysis was applied to better understand the correlation between immune cells and the m6AScore (Figure S4C and Table S23). m6AScore was found to be positively associated with regulatory T cell. To further shed light on the impact of m6AScore in AML, we next explored its potential value for

predicting clinical outcomes. Overall survival curves of Kaplan-Meier analyses revealed that patients with high m6Ascore had a significantly prominent prognosis ($P = 0.001$, Log-rank test, Figure 6B). Similarly, by univariate analyses of the TCGA data set, the high m6Ascore was significantly related to better OS (HR = 2.442, $P < 0.01$, Table S24). To explore the distribution variations of the somatic mutations between low and high m6Ascore, we evaluated samples from the TCGA dataset using the maftools package. The top five mutated genes in the high m6Ascore group were *CEBPA*, *KIT*, *FLT3*, *TET2*, and *NRAS*, in parallel, the top five mutated genes in the low m6Ascore group were *FLT3*, *DNMT3A*, *NPM1*, *IDH2*, and *IDH1* (Figure 6C, Figure 6D). The Forest plot revealed the alteration frequencies of the top five mutated genes in two groups using the chi-square test (Figure S4D). Delightfully, we found m6Ascore correlated strongly with tryptophan metabolism, pyruvate metabolism, glycogen degradation, cysteine and methionine metabolism, arachidonic acid metabolism, and ADP ribosylation (Figure 6E).

Discussion

As one of the most common, abundant, and intensively studied RNA modifications. m6A has been regarded as an important epigenetic mark that critically regulates RNA metabolism, cell signaling, cell survival, and differentiation which impacts the behavior and phenotype of cells [29, 30]. A recent wave of studies has provided critical insights that m6A modifications play an important part in leukemia [14–16, 31]. Nevertheless, most studies focus on the single regulator, and the overall role of multiple m6A regulators has not yet been fully elucidated. We aimed to characterize the association of integrated m6A modification patterns with TME which would offer us a deeper and richer understanding of the prognosis and development in AML.

Our study discovered that the relative abundance of 23 TILs closely correlated with the three m6A clusters, three m6A gene clusters, and m6Ascore. Nowadays, m6A modification has been found to play a critical role in tuning the immune response [32]. It is demonstrated that YTHDF1 is essential for durable neoantigen-specific immunity, and YTHDF1-deficient mice show an elevated antitumor response of tumor-infiltrating CD8⁺ T cell [33]. METTL3-mediated mRNA m6A modification participates in the physiological promotion of dendritic cell activation [34]. Indeed, leukemic blasts abnormally express the ligands for Immune Checkpoints (ICs) to escape immune supervision and present a series of metabolic alterations that could be involved in immunoregulation [35, 36].

The present study recognized evident features in 23 m6A regulators at the transcriptional and genetic levels in AML. We also constructed three distinct m6A methylation modification patterns based on 21 m6A regulators. Compared to patients with m6A cluster B and m6A cluster C, m6A cluster A group had a worse outcome. The characteristics of the GSVA enrichment analysis also differed significantly between the three subtypes. Our data showed that m6A cluster A was significantly enriched in metabolic pathways such as biosynthesis of unsaturated fatty acids, cysteine and methionine metabolism, and citrate cycle TCA cycle. It has been reported that METTL3 upregulates fatty acid synthase which reduces hepatic insulin sensitivity [37]. Additionally, METTL3 enhances lipid accumulation via downregulating peroxisome proliferator-activator α (PPAR α) expression [38]. In previous studies, methionine metabolism

was reported to be strongly related to m6A methylation [39]. And the free methionine can be converted to S-adenosylmethionine (SAM) [40]. Homeostatic regulation of SAM synthesis encompasses dynamic m6A modifications in the MAT2A 3' UTR of mammalian cells [41]. In recent years, the TCA cycle has also re-emerged as a pivotal metabolic hub that supports tumor growth in both mouse models of cancer and patients with cancer [42, 43].

Further, we identified three gene subtypes based on the DEGs between the three m6A clusters. The results concluded gene clusters could serve as valuable indexes for evaluating prognosis. In addition, m6A gene cluster A was prominently associated with metabolic pathways including glycogen degradation, and m6A gene cluster C presented enrichment pathways prominently associated with drug metabolism by cytochrome P450. Scholars have reported that R-2-hydroxyglutarate (R-2HG) abates FTO/m6A/YTHDF2-mediated upregulation of phosphofructokinase platelet (PFKP) and lactate dehydrogenase B (LDHB) which suppress aerobic glycolysis and exert an anti-tumor effect in R-2HG-sensitive leukemia cells [44]. Likewise, targeting FTO/MYC/CEBPA signaling, R-2HG displays an intrinsic and broad anti-tumor activity in leukemia [45]. On the same lines, Nakano M et al demonstrate that m6A modification regulates the expression level of drug-metabolizing enzymes P450 [46, 47]. And m6A modification affects drug and lipid metabolism by regulating the regulation of CES2 [48]. All of this verified again that the DEGs were deemed to be m6A phenotype-related gene signatures and the m6A modification played an important role in shaping different TME landscapes.

We next established a quantification system to define different m6A modification patterns of individual patients. Patients with low- and high-risk m6Ascores exhibited significantly different clinicopathological characteristics, prognosis, and mutation, respectively. What's more, m6Ascore correlated strongly with tryptophan metabolism, pyruvate metabolism, nicotinate, and nicotinamide metabolism, glycogen degradation, cysteine and methionine metabolism, arachidonic acid metabolism, ADP ribosylation, et al. Monocarboxylates such as lactate, pyruvate, and the ketone bodies play essential roles in metabolism [49]. As reported in the literature, pyruvate can be transformed into lactate via lactate dehydrogenase (LDH) which is frequently upregulated in multiple cancers [50]. Moreover, pyruvate carboxylase (PC) which is essential for primary and metastatic tumor growth catalyzes pyruvate to the TCA cycle metabolite oxaloacetate [51]. Wang et al. tested nicotinamide adenine dinucleotide phosphate (NADP) binds to FTO, which led to decreased m6A methylation in RNA and adipogenesis [52].

In this study, our comprehensive analysis based on 23 m6A regulators suggested the association of the m6A modification patterns with TME, clinicopathological features, and prognosis in AML. Moreover, various metabolic mechanisms related to the m6A's modification were discovered. Given metabolic reprogramming of tumor cells plays an extremely important role in tumor initiation and progression, focusing on m6A modification with altered metabolic pathways may be a promising anticancer strategy. In the same manner, elucidation of the significance of m6A in the regulation of the TME is expected to lead to a deeper understanding of the occurrence and development of AML.

Abbreviations

m6A
RNA N6-methyladenosine
TME
tumor microenvironment
AML
acute myeloid leukemia
DEGs
differentially expressed genes
TILs
tumor-infiltrating lymphocyte cells
METTL3
METTL3
METTL14
methyltransferase-like 14
ALKBH5
 α -ketoglutarate-dependent dioxygenase AlkB homolog 5
FTO
fat mass and obesity-associated protein
YTH
YT521-B homology
YTHDF2
YTH domain family protein 2
TCGA
the Cancer Genome Atlas
OS
overall survival
PCA
principal component analysis
RFE
recursive feature elimination
GSVA
Gene set variation analysis
CNV
copy number variation
ICs
Immune Checkpoints
PPAR α
peroxisome proliferator-activator
SAM
S-adenosylmethionine

R-2HG
R-2-hydroxyglutarate
PFKP
phosphofructokinase platelet
LDHB
lactate dehydrogenase B
LDH
lactate dehydrogenase
PC
pyruvate carboxylase
NADP
nicotinamide adenine dinucleotide phosphate

Declarations

Availability of data and materials

The data and R script files to reproduce figures contained within the manuscript are available.

Acknowledgements

The authors would like to offer sincere gratitude to the reviewers for their constructive comments on this article.

Funding

This study was supported by the National Natural Science Foundation of China (81970118, 81900163), Medical Innovation Team of Jiangsu Province (CXTDB2017002), Zhenjiang Clinical Research Center of Hematology (SS2018009), Social Development Foundation of Zhenjiang (SH2019065, SH2021052), Scientific Research Project of The Fifth 169 Project of Zhenjiang (21).

Author information

Zi-jun Xu, Xiang-mei Wen and Yuan-cui Zhang contributed equally to this work

Affiliations

Laboratory Center, Affiliated People's Hospital of Jiangsu University, Zhenjiang 212002, Jiangsu, P.R. China

Zi-jun Xu, Xiang-mei Wen, Ji-chun Ma, Xin-yi Chen, Pei-hui Xia & Jiang Lin

Zhenjiang Clinical Research Center of Hematology, Affiliated People's Hospital of Jiangsu University, Zhenjiang 212002, Jiangsu, P.R. China

Zi-jun Xu, Xiang-mei Wen, Ye Jin, Ji-chun Ma, Xin-yi Chen, Pei-hui Xia, Jiang Lin & Jun Qian

The Key Lab of Precision Diagnosis and Treatment in Hematologic Malignancies of Zhenjiang City, Affiliated People's Hospital of Jiangsu University, Zhenjiang 212002, Jiangsu, P.R. China

Zi-jun Xu, Xiang-mei Wen, Ji-chun Ma, Xin-yi Chen, Pei-hui Xia & Jiang Lin

Department of Internal Medicine, The Affiliated Third Hospital of Jiangsu University, Zhenjiang 212002, Jiangsu, P.R. China

Yuan-cui Zhang

Department of Hematology, Affiliated People's Hospital of Jiangsu University, Zhenjiang 212002, Jiangsu, P.R. China

Ye Jin, Yu Gu & Jun Qian

Department of Otolaryngology-Head and Neck Surgery, Affiliated People's Hospital of Jiangsu University, Zhenjiang 212002, Jiangsu, P.R. China

Wei Qian

Contributions

Jun Qian designed the research, Xiang-mei Wen and Ji-chun Ma organized and analyzed data, Zi-jun Xu, Ye Jin, Xin-yi Chen, and Pei-hui Xia prepared the figures and performed data analysis, Zi-jun Xu, Xiang-mei Wen, and Yu Gu drafted the manuscript, Jiang Lin and Wei Qian polished and revised the article. All authors read and approved the final manuscript.

Corresponding authors

Correspondence to Jun Qian, Jiang Lin or Wei Qian

Ethics declarations

Ethics approval and consent to participate

The present study was approved by the Ethics Committee of Affiliated People's Hospital of Jiangsu University (Approval Number: K-20190020-Y.)

Consent for publication

Not applicable.

Competing interests

The authors declare that there are no competing interests.

References

1. Dohner H, Estey E, Grimwade D, Amadori S, Appelbaum FR, Buchner T, Dombret H, Ebert BL, Fenaux P, Larson RA *et al*: **Diagnosis and management of AML in adults: 2017 ELN recommendations from an international expert panel.** *Blood* 2017, **129**(4):424-447.
2. Thomas D, Majeti R: **Biology and relevance of human acute myeloid leukemia stem cells.** *Blood* 2017, **129**(12):1577-1585.
3. Buckley SA, Kirtane K, Walter RB, Lee SJ, Lyman GH: **Patient-reported outcomes in acute myeloid leukemia: Where are we now?** *Blood Rev* 2018, **32**(1):81-87.
4. Koenig K, Mims A: **Relapsed or primary refractory AML: moving past MEC and FLAG-ida.** *Current opinion in hematology* 2020, **27**(2):108-114.
5. Metzeler KH, Herold T, Rothenberg-Thurley M, Amler S, Sauerland MC, Gorlich D, Schneider S, Konstandin NP, Dufour A, Braundl K *et al*: **Spectrum and prognostic relevance of driver gene mutations in acute myeloid leukemia.** *Blood* 2016, **128**(5):686-698.
6. Shi H, Wei J, He C: **Where, When, and How: Context-Dependent Functions of RNA Methylation Writers, Readers, and Erasers.** *Mol Cell* 2019, **74**(4):640-650.
7. Zhao BS, Roundtree IA, He C: **Post-transcriptional gene regulation by mRNA modifications.** *Nat Rev Mol Cell Biol* 2017, **18**(1):31-42.
8. Fu Y, Dominissini D, Rechavi G, He C: **Gene expression regulation mediated through reversible m(6)A RNA methylation.** *Nat Rev Genet* 2014, **15**(5):293-306.
9. Desrosiers R, Friderici K, Rottman F: **Identification of methylated nucleosides in messenger RNA from Novikoff hepatoma cells.** *Proceedings of the National Academy of Sciences of the United States of America* 1974, **71**(10):3971-3975.
10. Zaccara S, Ries RJ, Jaffrey SR: **Reading, writing and erasing mRNA methylation.** *Nat Rev Mol Cell Biol* 2019, **20**(10):608-624.
11. Vu LP, Cheng Y, Kharas MG: **The Biology of m(6)A RNA Methylation in Normal and Malignant Hematopoiesis.** *Cancer discovery* 2019, **9**(1):25-33.
12. Sheng Y, Wei J, Yu F, Xu H, Yu C, Wu Q, Liu Y, Li L, Cui XL, Gu X *et al*: **A Critical Role of Nuclear m6A Reader YTHDC1 in Leukemogenesis by Regulating MCM Complex-Mediated DNA Replication.** *Blood* 2021.
13. Paris J, Morgan M, Campos J, Spencer GJ, Shmakova A, Ivanova I, Mapperley C, Lawson H, Wotherspoon DA, Sepulveda C *et al*: **Targeting the RNA m(6)A Reader YTHDF2 Selectively Compromises Cancer Stem Cells in Acute Myeloid Leukemia.** *Cell stem cell* 2019, **25**(1):137-148 e136.
14. Vu LP, Pickering BF, Cheng Y, Zaccara S, Nguyen D, Minuesa G, Chou T, Chow A, Saletore Y, MacKay M *et al*: **The N(6)-methyladenosine (m(6)A)-forming enzyme METTL3 controls myeloid differentiation**

- of normal hematopoietic and leukemia cells. *Nature medicine* 2017, **23**(11):1369-1376.
15. Weng H, Huang H, Wu H, Qin X, Zhao BS, Dong L, Shi H, Skibbe J, Shen C, Hu C *et al*: **METTL14 Inhibits Hematopoietic Stem/Progenitor Differentiation and Promotes Leukemogenesis via mRNA m(6)A Modification**. *Cell stem cell* 2018, **22**(2):191-205 e199.
 16. Shen C, Sheng Y, Zhu AC, Robinson S, Jiang X, Dong L, Chen H, Su R, Yin Z, Li W *et al*: **RNA Demethylase ALKBH5 Selectively Promotes Tumorigenesis and Cancer Stem Cell Self-Renewal in Acute Myeloid Leukemia**. *Cell stem cell* 2020, **27**(1):64-80 e69.
 17. Barbieri I, Tzelepis K, Pandolfini L, Shi J, Millan-Zambrano G, Robson SC, Aspris D, Migliori V, Bannister AJ, Han N *et al*: **Promoter-bound METTL3 maintains myeloid leukaemia by m(6)A-dependent translation control**. *Nature* 2017, **552**(7683):126-131.
 18. Li Z, Weng H, Su R, Weng X, Zuo Z, Li C, Huang H, Nachtergaele S, Dong L, Hu C *et al*: **FTO Plays an Oncogenic Role in Acute Myeloid Leukemia as a N(6)-Methyladenosine RNA Demethylase**. *Cancer cell* 2017, **31**(1):127-141.
 19. Friedl P, Alexander S: **Cancer invasion and the microenvironment: plasticity and reciprocity**. *Cell* 2011, **147**(5):992-1009.
 20. Hanahan D, Weinberg RA: **Hallmarks of cancer: the next generation**. *Cell* 2011, **144**(5):646-674.
 21. Binnewies M, Roberts EW, Kersten K, Chan V, Fearon DF, Merad M, Coussens LM, Gaborilovich DI, Ostrand-Rosenberg S, Hedrick CC *et al*: **Understanding the tumor immune microenvironment (TIME) for effective therapy**. *Nature medicine* 2018, **24**(5):541-550.
 22. Li Z, Zhang H: **Reprogramming of glucose, fatty acid and amino acid metabolism for cancer progression**. *Cell Mol Life Sci* 2016, **73**(2):377-392.
 23. Faubert B, Li KY, Cai L, Hensley CT, Kim J, Zacharias LG, Yang C, Do QN, Doucette S, Burguete D *et al*: **Lactate Metabolism in Human Lung Tumors**. *Cell* 2017, **171**(2):358-371 e359.
 24. Choe J, Lin S, Zhang W, Liu Q, Wang L, Ramirez-Moya J, Du P, Kim W, Tang S, Sliz P *et al*: **mRNA circularization by METTL3-eIF3h enhances translation and promotes oncogenesis**. *Nature* 2018, **561**(7724):556-560.
 25. Mendez-Ferrer S, Bonnet D, Steensma DP, Hasserjian RP, Ghobrial IM, Gribben JG, Andreeff M, Krause DS: **Bone marrow niches in haematological malignancies**. *Nature reviews Cancer* 2020, **20**(5):285-298.
 26. Liu Y, Liang G, Xu H, Dong W, Dong Z, Qiu Z, Zhang Z, Li F, Huang Y, Li Y *et al*: **Tumors exploit FTO-mediated regulation of glycolytic metabolism to evade immune surveillance**. *Cell Metab* 2021, **33**(6):1221-1233 e1211.
 27. Zeng D, Li M, Zhou R, Zhang J, Sun H, Shi M, Bin J, Liao Y, Rao J, Liao W: **Tumor Microenvironment Characterization in Gastric Cancer Identifies Prognostic and Immunotherapeutically Relevant Gene Signatures**. *Cancer immunology research* 2019, **7**(5):737-750.
 28. Newman AM, Liu CL, Green MR, Gentles AJ, Feng W, Xu Y, Hoang CD, Diehn M, Alizadeh AA: **Robust enumeration of cell subsets from tissue expression profiles**. *Nature methods* 2015, **12**(5):453-457.

29. Meyer KD, Jaffrey SR: **Rethinking m(6)A Readers, Writers, and Erasers.** *Annu Rev Cell Dev Biol* 2017, **33**:319-342.
30. Roundtree IA, Evans ME, Pan T, He C: **Dynamic RNA Modifications in Gene Expression Regulation.** *Cell* 2017, **169**(7):1187-1200.
31. Elkashef SM, Lin AP, Myers J, Sill H, Jiang D, Dahia PLM, Aguiar RCT: **IDH Mutation, Competitive Inhibition of FTO, and RNA Methylation.** *Cancer cell* 2017, **31**(5):619-620.
32. Shulman Z, Stern-Ginossar N: **The RNA modification N(6)-methyladenosine as a novel regulator of the immune system.** *Nature immunology* 2020, **21**(5):501-512.
33. Han D, Liu J, Chen C, Dong L, Liu Y, Chang R, Huang X, Liu Y, Wang J, Dougherty U *et al*: **Anti-tumour immunity controlled through mRNA m(6)A methylation and YTHDF1 in dendritic cells.** *Nature* 2019, **566**(7743):270-274.
34. Wang H, Hu X, Huang M, Liu J, Gu Y, Ma L, Zhou Q, Cao X: **Mettl3-mediated mRNA m(6)A methylation promotes dendritic cell activation.** *Nature communications* 2019, **10**(1):1898.
35. Mougikakos D: **The Induction of a Permissive Environment to Promote T Cell Immune Evasion in Acute Myeloid Leukemia: The Metabolic Perspective.** *Frontiers in oncology* 2019, **9**:1166.
36. Toffalori C, Zito L, Gambacorta V, Riba M, Oliveira G, Bucci G, Barcella M, Spinelli O, Greco R, Crucitti L *et al*: **Immune signature drives leukemia escape and relapse after hematopoietic cell transplantation.** *Nature medicine* 2019, **25**(4):603-611.
37. Xie W, Ma LL, Xu YQ, Wang BH, Li SM: **METTL3 inhibits hepatic insulin sensitivity via N6-methyladenosine modification of Fasn mRNA and promoting fatty acid metabolism.** *Biochemical and biophysical research communications* 2019, **518**(1):120-126.
38. Zhong X, Yu J, Frazier K, Weng X, Li Y, Cham CM, Dolan K, Zhu X, Hubert N, Tao Y *et al*: **Circadian Clock Regulation of Hepatic Lipid Metabolism by Modulation of m(6)A mRNA Methylation.** *Cell reports* 2018, **25**(7):1816-1828 e1814.
39. Cao G, Li HB, Yin Z, Flavell RA: **Recent advances in dynamic m6A RNA modification.** *Open Biol* 2016, **6**(4):160003.
40. Anstee QM, Day CP: **S-adenosylmethionine (SAdMet) therapy in liver disease: a review of current evidence and clinical utility.** *Journal of hepatology* 2012, **57**(5):1097-1109.
41. Shima H, Matsumoto M, Ishigami Y, Ebina M, Muto A, Sato Y, Kumagai S, Ochiai K, Suzuki T, Igarashi K: **S-Adenosylmethionine Synthesis Is Regulated by Selective N(6)-Adenosine Methylation and mRNA Degradation Involving METTL16 and YTHDC1.** *Cell reports* 2017, **21**(12):3354-3363.
42. Krall AS, Mullen PJ, Surjono F, Momcilovic M, Schmid EW, Halbrook CJ, Thambundit A, Mittelman SD, Lyssiotis CA, Shackelford DB *et al*: **Asparagine couples mitochondrial respiration to ATF4 activity and tumor growth.** *Cell Metab* 2021, **33**(5):1013-1026 e1016.
43. Martinez-Reyes I, Cardona LR, Kong H, Vasan K, McElroy GS, Werner M, Kihshen H, Reczek CR, Weinberg SE, Gao P *et al*: **Mitochondrial ubiquinol oxidation is necessary for tumour growth.** *Nature* 2020, **585**(7824):288-292.

44. Qing Y, Dong L, Gao L, Li C, Li Y, Han L, Prince E, Tan B, Deng X, Wetzel C *et al*: **R-2-hydroxyglutarate attenuates aerobic glycolysis in leukemia by targeting the FTO/m(6)A/PFKP/LDHB axis.** *Mol Cell* 2021, **81**(5):922-939 e929.
45. Su R, Dong L, Li C, Nachtergaele S, Wunderlich M, Qing Y, Deng X, Wang Y, Weng X, Hu C *et al*: **R-2HG Exhibits Anti-tumor Activity by Targeting FTO/m(6)A/MYC/CEBPA Signaling.** *Cell* 2018, **172**(1-2):90-105 e123.
46. Nakano M, Nakajima M: **A-to-I RNA editing and m(6)A modification modulating expression of drug-metabolizing enzymes.** *Drug Metab Dispos* 2022.
47. Nakano M, Ondo K, Takemoto S, Fukami T, Nakajima M: **Methylation of adenosine at the N(6) position post-transcriptionally regulates hepatic P450s expression.** *Biochem Pharmacol* 2020, **171**:113697.
48. Takemoto S, Nakano M, Fukami T, Nakajima M: **m(6)A modification impacts hepatic drug and lipid metabolism properties by regulating carboxylesterase 2.** *Biochem Pharmacol* 2021, **193**:114766.
49. Halestrap AP: **Monocarboxylic acid transport.** *Compr Physiol* 2013, **3**(4):1611-1643.
50. Wang ZY, Loo TY, Shen JG, Wang N, Wang DM, Yang DP, Mo SL, Guan XY, Chen JP: **LDH-A silencing suppresses breast cancer tumorigenicity through induction of oxidative stress mediated mitochondrial pathway apoptosis.** *Breast Cancer Res Treat* 2012, **131**(3):791-800.
51. Christen S, Lorendeau D, Schmieder R, Broekaert D, Metzger K, Veys K, Elia I, Buescher JM, Orth MF, Davidson SM *et al*: **Breast Cancer-Derived Lung Metastases Show Increased Pyruvate Carboxylase-Dependent Anaplerosis.** *Cell reports* 2016, **17**(3):837-848.
52. Wang L, Song C, Wang N, Li S, Liu Q, Sun Z, Wang K, Yu SC, Yang Q: **NADP modulates RNA m(6)A methylation and adipogenesis via enhancing FTO activity.** *Nat Chem Biol* 2020, **16**(12):1394-1402.

Figures

Figure 1

The panorama of genetic variations and expression patterns of m6A regulators in AML. (A) The CNV variation frequency of 23 m6A regulators was prevalent from the TCGA cohort. The height of the column denoted the alteration frequency. The amplification frequency was labeled as a red dot. The deletion frequency was labeled as a blue dot. (B) The location of CNV alteration of m6A regulators on chromosomes. The black dot, the red dot, and the blue dot in the ring indicated no copy number change, amplification, and deletion respectively. (C) The genetic alteration frequency of 23 m6A regulators in 193 patients with AML. The upper bar plot showed TMB. The panel on the right represented the mutation frequency and proportion of each variant type in each regulator. (D) Correlation of the investigated m6A modification regulators. (E) The differences of expression levels of 23 m6A regulators between normal and AML samples (***) $P < 0.001$.

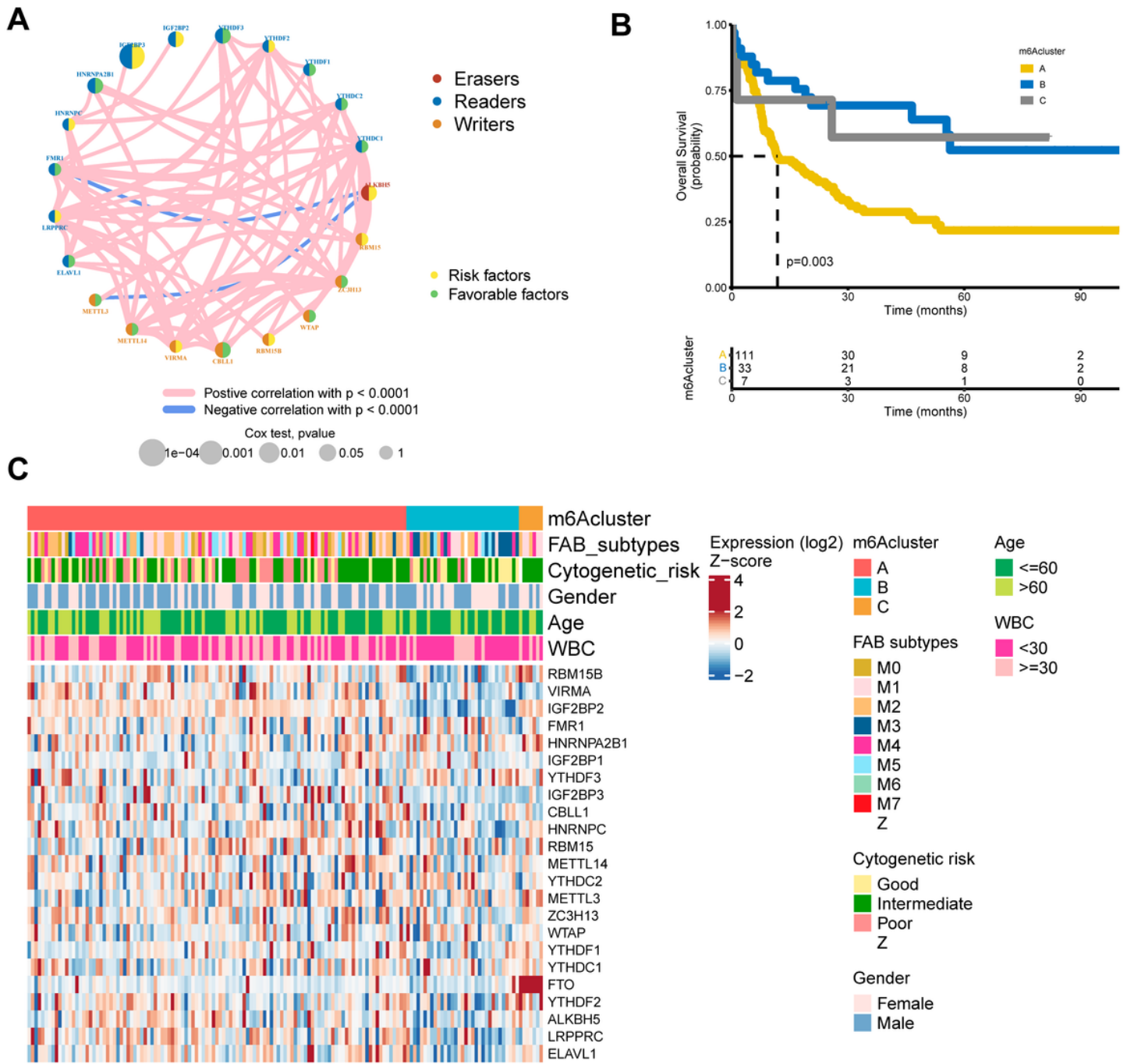


Figure 2

m6A regulators subtypes and their clinicopathological characteristics in AML. (A) The interaction among m6A regulators in AML. The lines represented their interactions between regulators, and the thickness of lines showed the strength of the correlation. Effects of regulators on the prognosis were represented with the circle size, and P -values were calculated by Log-rank test ($P < 1$, $P < 0.05$, $P < 0.01$, $P < 0.001$, $P < 1e^{-04}$). (B) Kaplan–Meier overall survival curves of 111 cases in m6A cluster A, 33 cases in m6A cluster B, and 7 cases in m6A cluster C. (C) Differences in clinicopathological characteristics and expression levels

of m6A among the three distinct m6A clusters. The m6A cluster, FAB subtypes, cytogenetic risk, gender, age, and WBC were used as patient annotations.

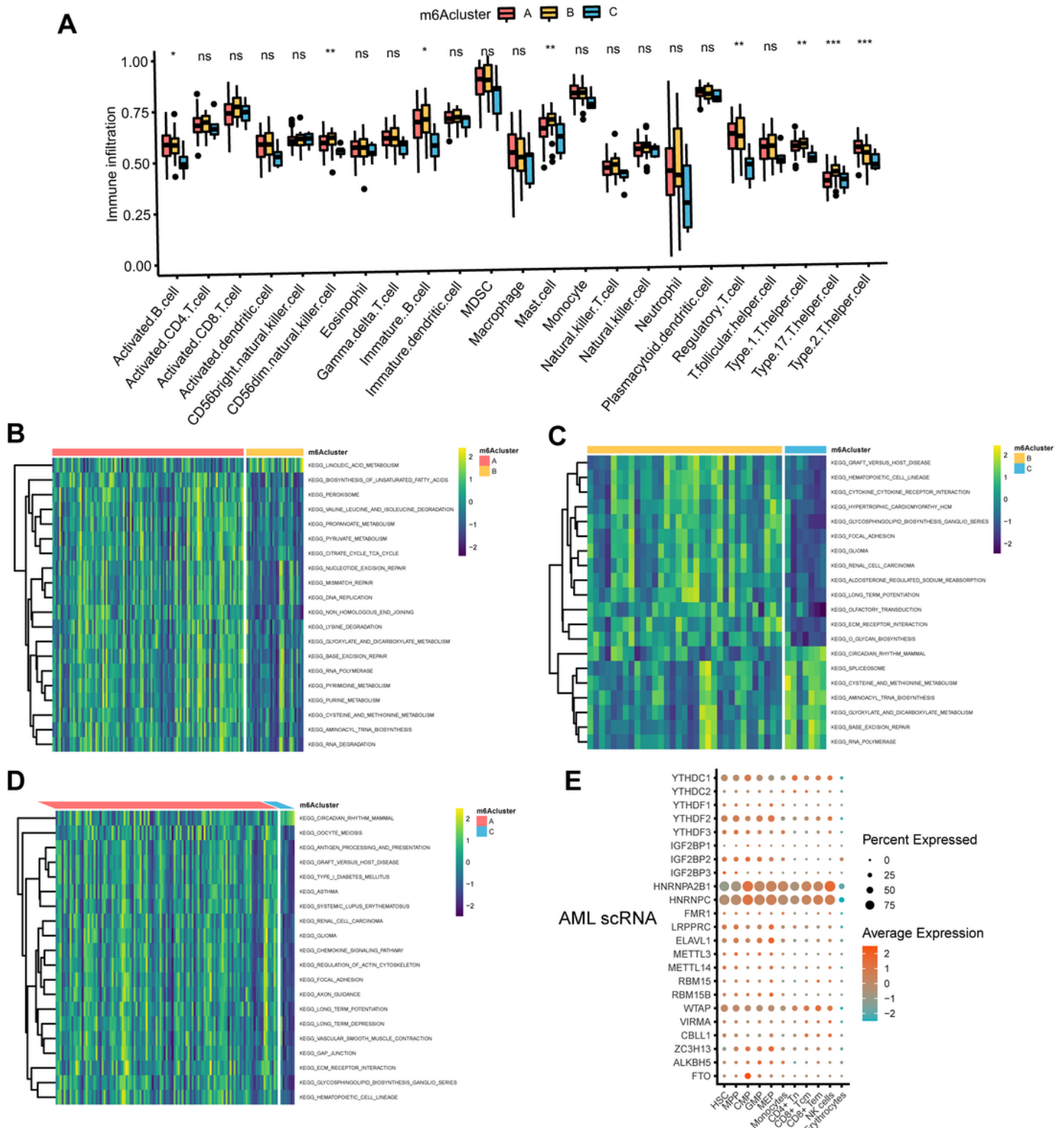


Figure 3

The interaction between TME and three m6A subtypes. (A) The abundance of tumor-infiltrating lymphocyte cells in three m6A clusters. Violin plots displayed the differences in the immune cell

distribution across three distinct subtypes. * $P < 0.05$, ** $P < 0.01$, *** $P < 0.01$, ns, not significant. (B-D) GSVA enrichment analysis of biological pathways in three distinct subtypes, visualized by the heatmap. B, m6Acluster A vs m6Acluster B, C, m6Acluster B vs m6Acluster C, D, m6Acluster A vs m6Acluster C. (E) Dot plot of cell type assignment for AML scRNA expressed genes. Dot plot charts of the average expression were shown in different colors, and the percentage of cells with detectable expression was demonstrated in the size of the dot.

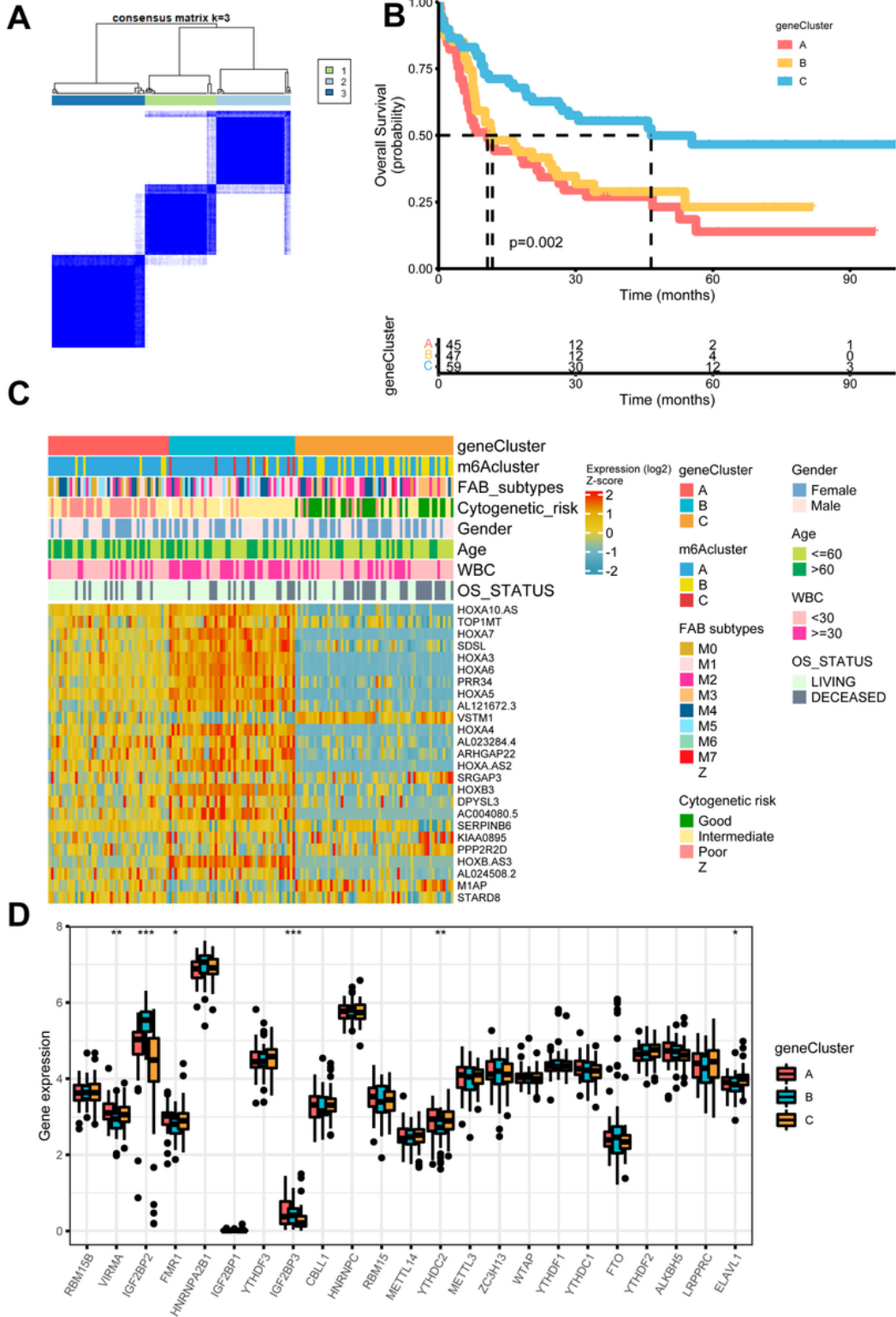


Figure 4

Construction of differential expression of m6A gene signatures. (A) Unsupervised clustering of m6A phenotype-related genes in the TCGA cohort and consensus matrices for $k = 3$. (B) Kaplan–Meier curves for overall survival of the m6A phenotype-related gene signatures ($P = 0.002$, Log-rank test). (C) Relationships between clinicopathologic features and the three genomic subtypes. The gene clusters, m6A clusters, FAB subtypes, cytogenetic risk, gender, age, white blood cell, and overall survival status were used as patient annotations. (D) Differences in the expression of 23 m6A regulators in the three gene clusters. * $P < 0.05$, ** $P < 0.01$, *** $P < 0.001$.

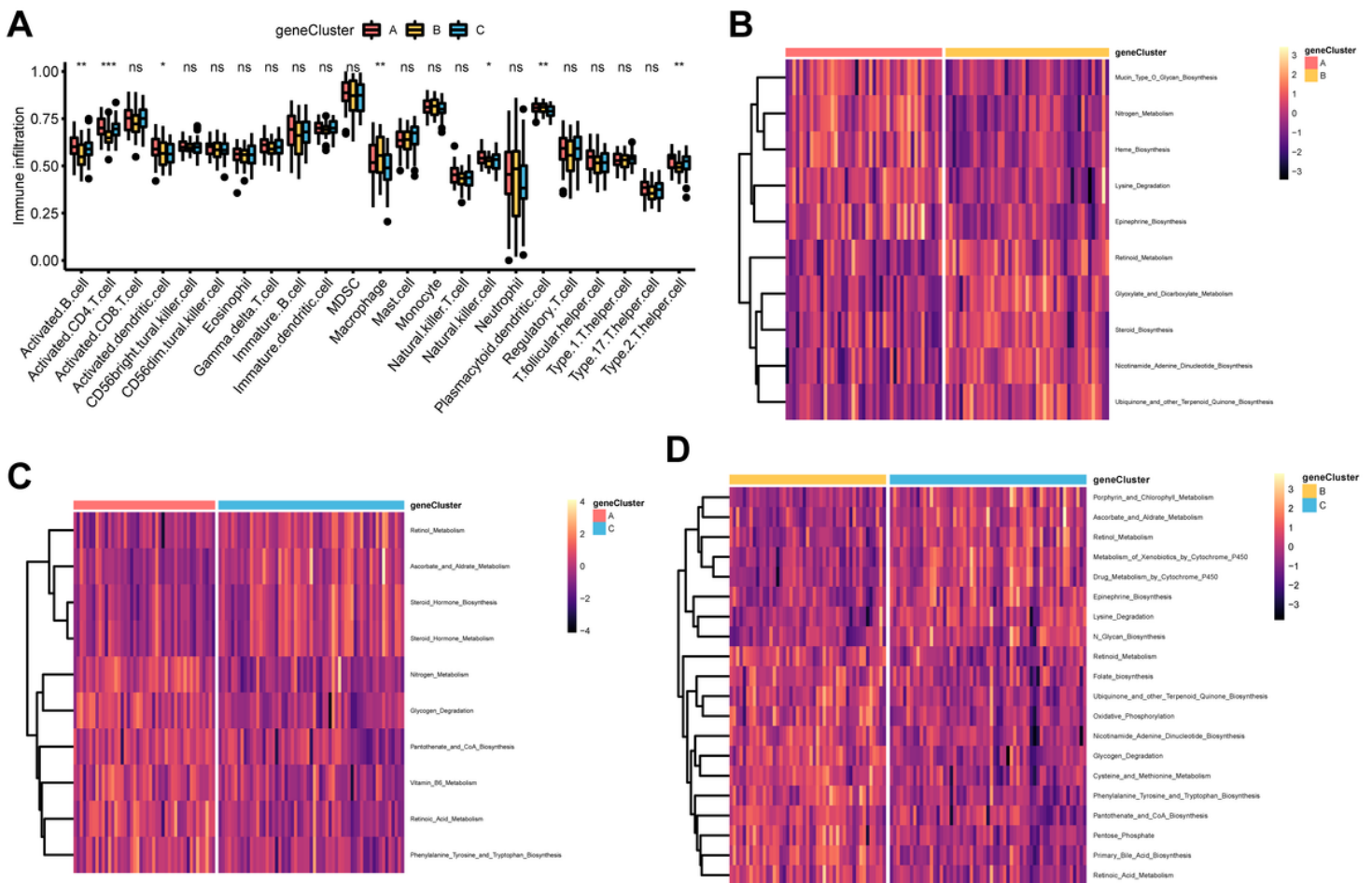


Figure 5

Correlations of TME and three m6A gene clusters. (A) The fraction of tumor-infiltrating lymphocyte cells in three m6A gene clusters using the CIBERSORT algorithm. Violin plots illustrated the differences in the immune cell distribution across three m6A gene clusters. * $P < 0.05$, ** $P < 0.01$, *** $P < 0.01$, ns, not significant. (B-D) Heatmap was plotted to show the activation states of biological pathways in three m6A gene clusters via the GSVA enrichment analysis. B, m6A gene cluster A vs m6A gene cluster B, C, m6A gene cluster B vs m6A gene cluster C, D, m6A gene cluster A vs m6A gene cluster C.

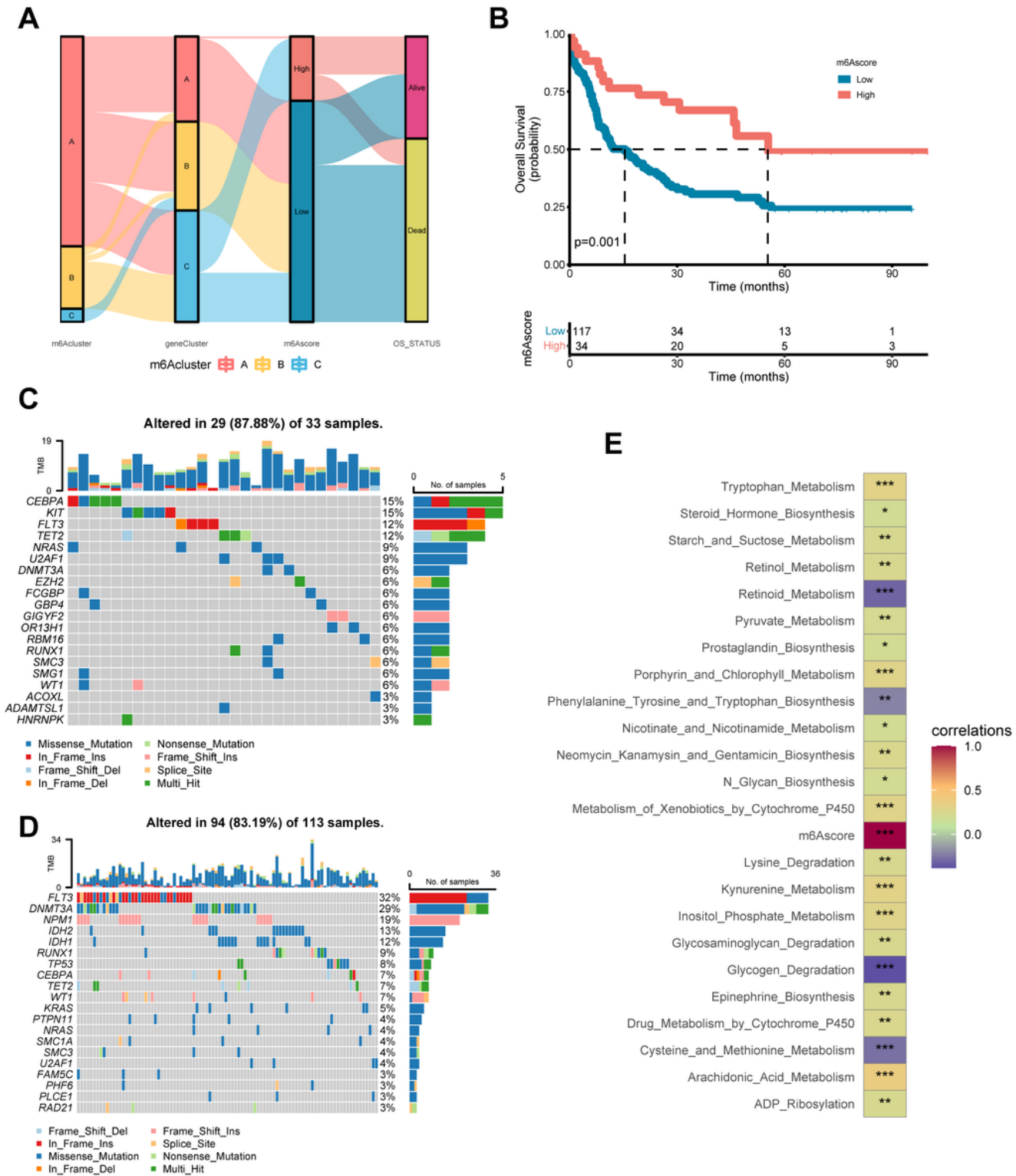


Figure 6

Construction of the m6A score in the training set and the relevance of clinical features. (A) Alluvial diagram of subtype distributions in groups with different m6A clusters, m6A gene clusters, m6A score, and OS status. (B) Kaplan-Meier analysis for high m6A score and low m6A score groups in AML cohort ($P = 0.001$, Log-rank test). (C-D) OncoPrint visualized the frequently mutated genes in the high m6AScore group (C) and the low m6AScore group (D). In the above two figures, the top 20 mutated genes were

distributed vertically by reducing mutation frequency from top to bottom. (E) Functional annotation for m6Ascore using GSVA enrichment analysis. The intensity of the colors represents the strength of correlation.

Supplementary Files

This is a list of supplementary files associated with this preprint. Click to download.

- [FigureS1.tif](#)
- [FigureS2.tif](#)
- [FigureS3.tif](#)
- [FigureS4.tif](#)
- [SupplementaryTables.xlsx](#)